

THERMAL FRACTURE OF CERAMICS WITH TEMPERATURE-DEPENDENT PROPERTIES

Z.-H. Jin and R. C. Batra

Department of Engineering Science and Mechanics
Virginia Polytechnic Institute and State University
Blacksburg, Virginia, USA

Some aspects of thermal fracture mechanics of ceramics with temperature-dependent properties are studied. It is first shown that the square-root singular field still prevails in the crack tip region. However, the size of the K-dominant zone may be influenced by the effect of temperature-dependent properties. Then the steady thermal stress intensity factor in an edge-cracked strip is calculated. The results show that the stress intensity factor, which is zero when the temperature dependence of material properties is neglected, can exceed the fracture toughness of the ceramic when the temperature dependence of the material properties is considered. Finally, a temperature-dependent crack-bridging law is proposed to study the R-curve behavior of polycrystalline ceramics subjected to elevated temperatures.

Keywords crack-bridging, fracture toughness, R-curve, thermal stress, thermal stress intensity factor

Material properties, such as the modulus of elasticity and the thermal conductivity, vary with temperature. These properties are usually regarded as constants in thermal stress analyses of engineering materials and structures, which is approximately correct when the temperature variation from the initial temperature is not very high. The structural components used in reactor vessels, turbine engines, space vehicles, and refractory industries are exposed to high temperature changes. In the thermal stress analyses of these components, neglecting the temperature dependence of material properties will usually result in significant errors. Extensive studies have been conducted on thermal stresses in materials with temperature-dependent properties, and most of those completed by the early 1990s have been reviewed by Noda [1, 2]. However, only a little effort has been devoted to analyzing the thermal fracture of materials with temperature-dependent properties. Hata [3, 4] studied steady thermal stress intensity factors at a central crack in an infinite plate using a perturbation technique. The temperature dependence of the shear modulus, the coefficient of thermal expansion, and thermal conductivity was included in his analysis. Kokini [5] used the finite element method to calculate transient thermal stress intensity factors in a cracked strip with temperature-dependent thermal properties.

Received 11 June 1997; accepted 14 October 1997.

Address correspondence to Romesh C. Batra, Department of Engineering Science & Mechanics, Virginia Polytechnic Institute and State University, Blacksburg, VA 24061-0219.

Journal of Thermal Stresses, 21:157-176, 1998
Copyright © 1998 Taylor & Francis
0149-5739/98 \$12.00 + .00

We study here some aspects of thermal fracture mechanics of ceramics with temperature-dependent properties. We first investigate the asymptotic expressions of the crack tip temperature and stress fields and the dominant zone of the asymptotic solutions. Then, the steady thermal stresses and stress intensity factors in an edge-cracked strip with temperature-dependent Young's modulus, the coefficient of thermal expansion, and thermal conductivity are calculated. Finally, the effect of temperature-dependent crack-face-grain-bridging on the crack growth resistance curve (*R*-curve) of a ceramic is explored and the crack growth instability analyzed.

CRACK TIP FIELDS IN MATERIALS WITH TEMPERATURE-DEPENDENT PROPERTIES

Basic Equations

A homogeneous material with temperature-dependent properties becomes nonhomogeneous when subjected to temperature changes. The basic equations, in rectangular Cartesian coordinates, governing the Airy stress function, F , and temperature, T , for nonhomogeneous linear elastic materials undergoing plane strain deformations are [6]

$$\frac{1-\nu^2}{E} \nabla^2 \nabla^2 F + \left(\frac{1-\nu^2}{E} \right)_{,i} (\nabla^2 F)_{,i} + \nabla^2 \left(\frac{1-\nu^2}{E} \right) \nabla^2 F + \left(\frac{1+\nu}{E} \right)_{,ij} (\delta_{ij} \nabla^2 F - F_{,ij}) + \nabla^2 [(1+\nu)\alpha(T-T_0)] = 0 \quad (1)$$

$$\nabla^2 T + \frac{1}{k} k_{,i} T_{,i} = \frac{1}{\kappa} \frac{\partial T}{\partial t} \quad (2)$$

where E is Young's modulus, ν Poisson's ratio, α the coefficient of thermal expansion, k the thermal conductivity, κ the thermal diffusivity, T_0 a reference temperature, and ∇^2 the two-dimensional Laplace operator. Since all material properties are functions of temperature, the derivatives of the properties in Eqs. (1) and (2) are

$$\left(\frac{1-\nu^2}{E} \right)_{,i} = \frac{d}{dT} \left(\frac{1-\nu^2}{E} \right) T_{,i} \quad (3)$$

$$\nabla^2 \left(\frac{1-\nu^2}{E} \right) = \frac{d}{dT} \left(\frac{1-\nu^2}{E} \right) \nabla^2 T + \frac{d^2}{dT^2} \left(\frac{1-\nu^2}{E} \right) T_{,i} T_{,i}$$

$$\frac{1+\nu}{E} = \frac{d}{dT} \left(\frac{1+\nu}{E} \right) T_{,ij} + \frac{d^2}{dT^2} \left(\frac{1+\nu}{E} \right) T_{,i} T_{,j} \quad (3)$$

$$k_{,i} = \frac{dk}{dT} T_{,i} \quad (\text{Cont.})$$

In Eqs. (1) to (3), the indices i and j take values 1 and 2, δ_{ij} is the Kronecker delta, a repeated index implies summation over the range of the index, and a comma followed by the index i implies partial differentiation with respect to x_i . Equation (3) implies that the gradients of the material properties may be singular at a crack tip because the heat flux (proportional to the temperature gradient) is generally singular. This is different from conventional nonhomogeneous materials wherein the gradients of material properties are finite. Also, Eq. (2) is nonlinear in temperature.

Temperature Fields

We first note that the heat flow across any finite arc is finite. Hence, the singularity of the heat flux at a crack tip is weaker than r^{-1} , where r is the distance from the crack tip. One can show that at a crack tip ($r \rightarrow 0$) the temperature and the heat flux have the following asymptotic forms:

$$T(r, \theta, t) = T_{\text{tip}}(t) - \frac{K_Q(t)}{k_{\text{tip}}} \sqrt{\frac{2r}{\pi}} \sin \frac{\theta}{2} \quad (4)$$

$$(q_r, q_\theta) = \frac{K_Q(t)}{\sqrt{2\pi r}} \left(\sin \frac{\theta}{2}, \cos \frac{\theta}{2} \right) \quad (5)$$

where q_r and q_θ are heat fluxes in the radial and tangential directions, (r, θ) are polar coordinates centered at the crack tip with the crack faces being $\theta = \pm \pi$, $T_{\text{tip}}(t)$ is the temperature at the crack tip, k_{tip} the thermal conductivity at the crack tip, and $K_Q(t)$ is the heat flux intensity. Equations (4) and (5) have the same form as those for materials in which effects of the temperature dependence of material properties [7] are neglected.

Stress and Deformation Fields

It can be seen from Eqs. (1) and (3) to (5) that the crack tip dominant solution for the stress function still satisfies a biharmonic equation. Hence, the square-root singular stress field prevails in the crack tip region

$$\sigma_{ij}(r, \theta, t) = \frac{1}{\sqrt{2\pi r}} \{ K_I \tilde{\sigma}_{ij}^{(1)}(\theta) + K_{II} \tilde{\sigma}_{ij}^{(2)}(\theta) \} \quad (6)$$

and the energy release rate

$$G = \frac{1 - \nu_{\text{tip}}^2}{E_{\text{tip}}} (K_I^2 + K_{II}^2) \quad (7)$$

Here E_{tip} and ν_{tip} are the Young's modulus and Poisson's ratio at the crack tip. They usually differ from their values at the room temperature.

Though the square-root singular field (6) is not influenced by the variations of material properties with temperature, the size of the region in which Eq. (6) holds (K -dominant zone) will be affected. Jin and Batra [8] have given the following approximate K -dominance condition for general nonhomogeneous materials

$$E^{-1}|E| \ll r^{-1} \quad E^{-1}|E_{,ij}| \ll r^{-2} \quad (8)$$

For temperature-dependent material properties, the gradients of properties are given in Eq. (3). Substituting Eq. (3) into Eq. (8) and considering the heat flux field (5), we have

$$\frac{1}{E} \left| \frac{dE}{dT} \right| \frac{|K_Q|}{k_{\text{tin}}} \ll \sqrt{\frac{2\pi}{r}} \quad \frac{1}{E} \left| \frac{d^2E}{dT^2} \right| \left(\frac{K_Q}{k_{\text{tip}}} \right)^2 \ll \frac{2\pi}{r} \quad (9)$$

The crack tip plastic deformation at room temperature is extremely limited in ceramics. At high temperatures, however, some plastic deformation may occur. Under small-scale yielding conditions, the crack tip plastic zone size is approximately given by (Mode I, plane strain)

$$r_p = \frac{1}{2\pi} \left(\frac{K_I}{\sigma_{ys}} \right)^2 \quad (10)$$

where σ_{ys} is the temperature-dependent yield stress. For polycrystalline ceramics, a microcracking zone may exist near the crack tip [9, 10]. The approximate size of the crack tip microcracking zone may again be given by Eq. (10) with σ_{ys} replaced by σ_{mc} , the stress at which microcracking occurs [11]. Therefore, in order for a K -dominant zone to exist at the crack tip, Eq. (9) should hold where $r > r_p$. For isotropic materials with temperature-dependent properties, this condition may also be approximated as

$$\frac{1}{E} \left| \frac{dE}{dT} \right| \frac{|K_Q|}{k_{\text{tip}}} \ll 2\pi \frac{\sigma_{ys}}{K_I} \quad \frac{1}{E} \left| \frac{d^2E}{dT^2} \right| \left(\frac{K_Q}{k_{\text{tip}}} \right)^2 \ll (2\pi)^2 \left(\frac{\sigma_{ys}}{K_I} \right)^2 \quad (11)$$

THERMAL STRESSES IN A STRIP

Henceforth, we evaluate the thermal stress and the thermal stress intensity factor in an edge-cracked strip subjected to steady heat flux in the thickness (cracking) direction. It is typical of problems in structural applications and allows a detailed discussion of the effects of temperature-dependent material properties. As will be seen in this article, in contrast to no stresses in the strip with temperature-independent properties, the steady thermal stress is significantly high and the stress intensity factor may exceed the fracture toughness of the material when temperature-dependent material properties are considered.

Temperature Field

Consider an infinite strip of width b , similar to that shown in Figure 1, subjected to steady temperatures T_0 and T_b ($T_b > T_0$) at the surfaces $x_1 = 0$ and $x_1 = b$, respectively. This problem is one-dimensional since the heat conducts only in the x_1 -direction. Thus, the temperature field is a solution of

$$\frac{d}{dx_1} \left[k(T) \frac{dT}{dx_1} \right] = 0 \quad (12)$$

$$T(0) = T_0 \quad T(b) = T_b \quad (13)$$

We approximate the variation of thermal conductivity with temperature by an affine function

$$k(T) = k_0[1 - \delta'(T - T_0)] \quad (14)$$

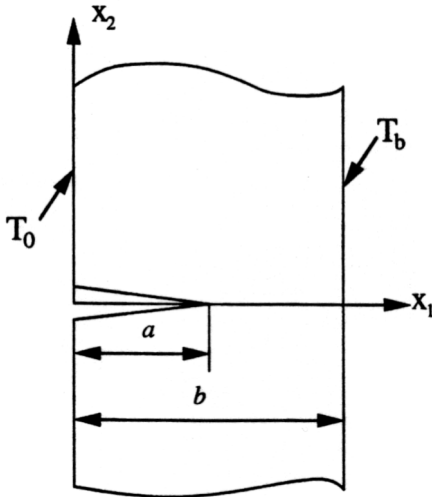


Figure 1. An infinite strip containing an edge crack

where k_0 is the thermal conductivity at $T = T_0$ and δ' is a constant. For typical ceramics, $0.3 \times 10^{-3} K^{-1} < \delta' < 0.8 \times 10^{-3} K^{-1}$ when the temperature does not exceed 1300 K [12]. It is common to model the temperature dependence of material properties [1] by affine functions. The temperature field obtained from Eqs. (12) to (14) is given by

$$(T - T_0) = \frac{1}{\delta'} \left[\left(\frac{1}{\delta'} \right)^2 - \Delta T \left(\frac{2}{\delta'} - \Delta T \right) \frac{x_1}{b} \right]^{1/2}$$

where $\Delta T = T_b - T_0$. The temperature is a nonlinear function of ΔT .

Thermal Stress

The temperature field (15) induces normal stresses in both the x_2 - and x_3 -directions in the strip. We assume that the strip undergoes plane strain deformations in the $(x_1 - x_2)$ -plane and is free from constraints at the far away ends. The stress in the x_2 -direction is [13]

$$\sigma_{22} = -\frac{E\alpha}{1-\nu}(T - T_0) + \frac{E}{(1-\nu^2)A_0} \left[(A_{22} - x_1 A_{12}) \int_0^b \frac{E\alpha}{1-\nu}(T - T_0) dx_1 - (A_{12} - x_1 A_{11}) \int_0^b \frac{E\alpha}{1-\nu}(T - T_0)x_1 dx_1 \right] \quad (16)$$

where A_{ij} ($i, j = 1, 2$) and A_0 are given in the appendix.

We assume that Poisson's ratio is constant and approximate Young's modulus and the *coefficient of thermal expansion* (CTE) again by affine functions

$$E(T) = E_0[1 - \beta'(T - T_0)]$$

$$\alpha(T) = \alpha_0[1 + \gamma'(T - T_0)]$$

where E_0 and α_0 are Young's modulus, the CTE at $T = T_0$, and β' and γ' are constants. For typical ceramics, $0.1 \times 10^{-3} K^{-1} < \beta' < 0.4 \times 10^{-3} K^{-1}$ and $0.1 \times 10^{-3} K^{-1} < \gamma' < 0.5 \times 10^{-3} K^{-1}$ when the temperature does not exceed 1300 K [12]. Figure 2 shows variations of E , α , and k with the temperatures for three different values of β , γ , and δ , which are related to β' , γ' , and δ' by

$$\beta, \delta, \gamma = (\beta', \delta', \gamma')800 \text{ K} \quad (19)$$

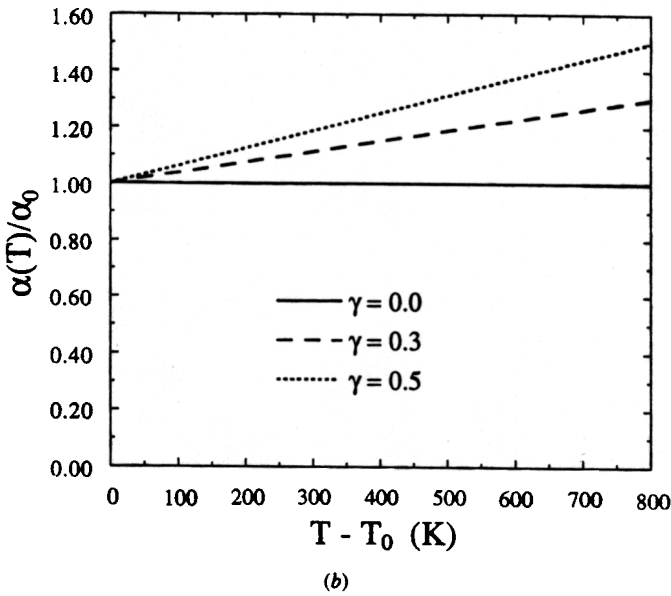
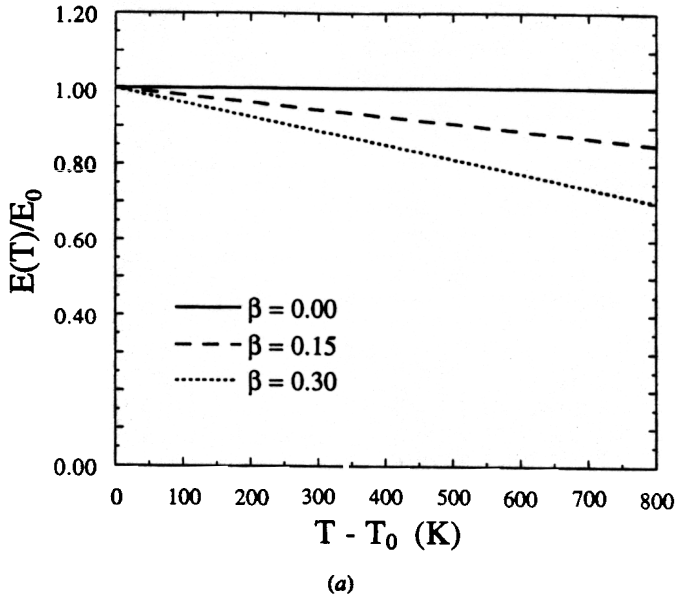


Figure 2. Variations of E , α , and k with temperature T for different values of β , γ , and δ .

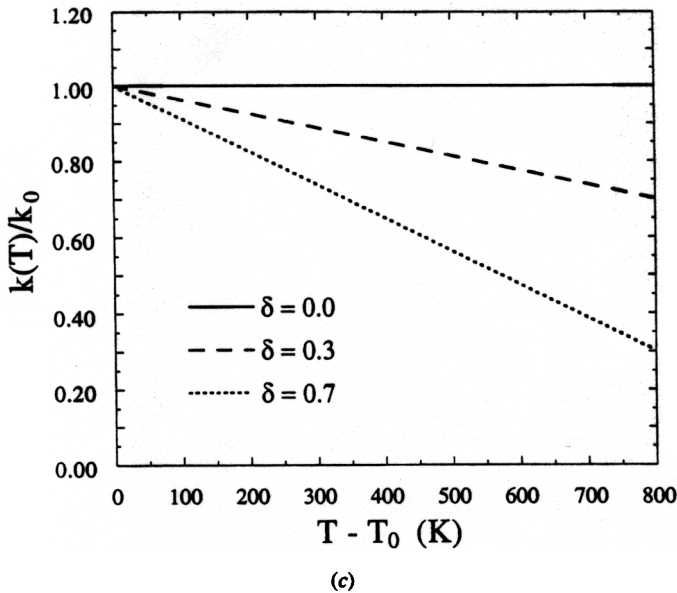


Figure 2. Variations of E , α , and k with temperature T for different values of β , γ , and δ (Continued).

Substituting Eqs. (15), (17), and (18) into Eq. (16), we obtain the normalized thermal stress

$$\begin{aligned} \frac{(1 - \nu_0) \sigma_{22}^T(x_1)}{E_0 \alpha_0 \Delta T} = & -[1 - \beta'(T - T_0)][1 + \gamma'(T - T_0)](T - T_0)/\Delta T \\ & + \frac{1 - \beta'(T - T_0)}{\tilde{A}_0} \left[\left(\tilde{A}_{22} - \frac{x_1}{b} \tilde{A}_{12} \right) I_1 - \left(\tilde{A}_{12} - \frac{x_1}{b} \tilde{A}_{11} \right) I_2 \right] \end{aligned} \quad (20)$$

where \tilde{A}_{ij} ($i, j = 1, 2$), \tilde{A}_0 , and I_i ($i = 1, 2$) are given in the appendix.

The thermal stress in the strip will vanish when the temperature dependence of material properties is neglected. Similarly, when one considers the temperature dependence of Young's modulus and ignores the temperature dependence of thermal properties (corresponding to $\beta' \neq 0$ and $\delta' = \gamma' = 0$ in Eqs. (14), (17), and (18)), the thermal stress is also zero.

Figure 3 shows the normalized thermal stress for $(\delta, \gamma) = (0.7, 0.5)$ and $\beta = 0.0, 0.15, 0.30$. Since the thermal stress is a nonlinear function of ΔT , we take $\Delta T = 800$ K here and in all subsequent calculations. It can be seen from Figure 3 that the

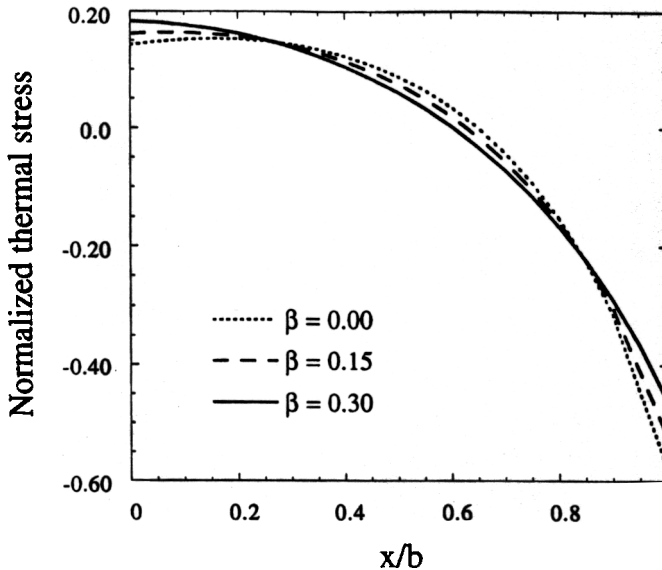
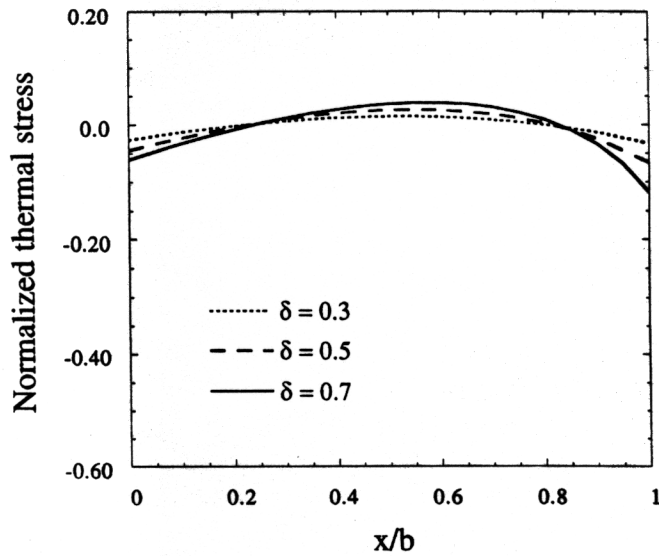
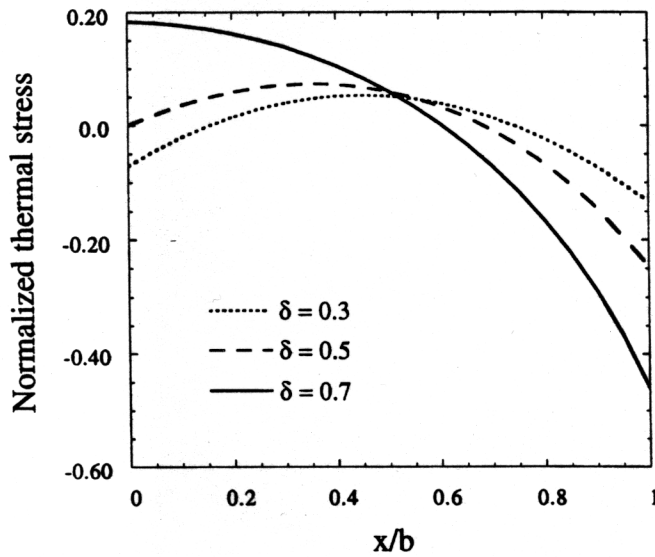


Figure 3. Normalized thermal stress in a strip for $\beta = 0, 0.15, 0.30$ and $\delta = 0.7, \gamma = 0.5$.

thermal stress is tensile on the low-temperature side ($x_1 = 0$) and compressive on the high-temperature side ($x_1 = b$). The maximum tensile stress occurs near or at $x_1 = 0$. The influence of parameter β on the thermal stress is insignificant. It seems that neglecting the temperature dependence of Young's modulus (described by β) will not cause significant errors in thermal stresses. When using the material properties $E_0 = 300$ GPa, $\nu_0 = 0.25$, $\alpha_0 = 3 \times 10^{-6} \text{ K}^{-1}$ for a silicon nitride ceramic (Si_3N_4), the maximum tensile stress for $(\beta, \delta, \gamma) = (0.3, 0.7, 0.3)$ with $\Delta T = 800$ K is about 92 MPa, which is high and must be considered along with the mechanically induced stresses. Figures 4a, b show the normalized thermal stress for $\delta = 0.3, 0.5, 0.7$ and $(\beta, \gamma) = (0.0, 0.0)$ (Figure 4a) and $(0.3, 0.5)$ (Figure 4b). It is seen from Figure 4a that the thermal stress is tensile in the interior of the plate and compressive at the plate surfaces. A similar result was obtained by Ganguly et al. [14], who only considered temperature-dependent thermal conductivity. It is evident in Figure 4b that the thermal stress varies dramatically with δ . Larger δ causes both higher tensile stress at $x_1 = 0$ and severe compressive stress at $x_1 = b$. However, when only the temperature dependence of thermal conductivity is considered, the magnitude of the thermal stress is small; the magnitude becomes large when the combined effects of the temperature dependence of the thermal conductivity and the coefficient of thermal expansion are considered. Figures 5a, b depict the normalized thermal stress for $\gamma = 0.1, 0.3, 0.5$ and $(\beta, \delta) = (0.0, 0.0)$ (Figure 5a) and $(0.3, 0.7)$ (Figure 5b). It is clear from Figure 5a that the stress distribution is symmetric about $x_1 = b/2$ when only the temperature dependence of the CTE is considered.



(a)



(b)

Figure 4. Normalized thermal stress in a strip for $\delta = 0.3, 0.5, 0.7$ and (a) $\beta = 0.0, \gamma = 0.0$ and (b) $\beta = 0.3, \gamma = 0.5$.

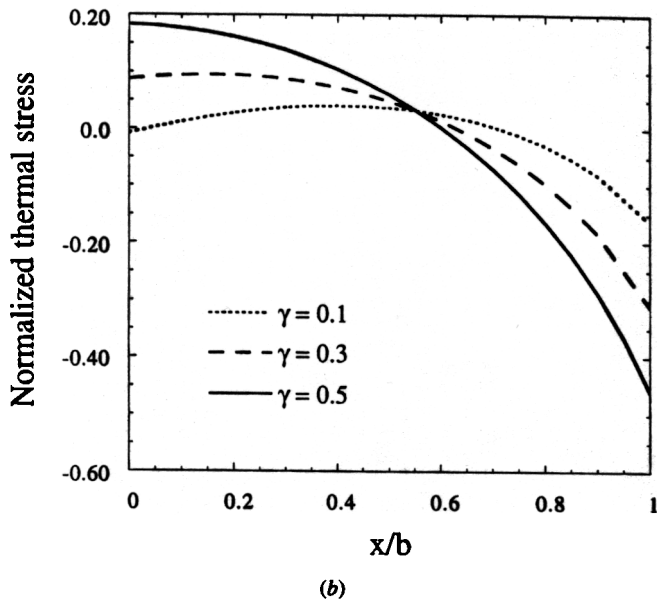
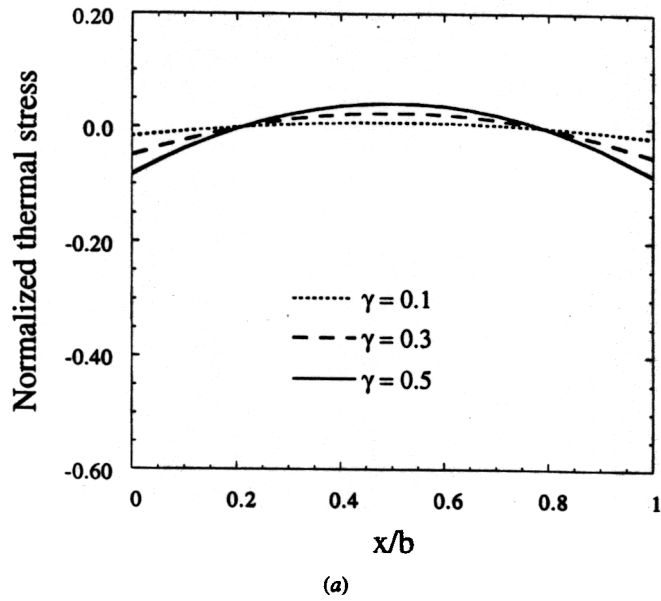


Figure 5. Normalized thermal stress in a strip for $\gamma = 0.1, 0.3, 0.5$ and (a) $\beta = 0.0, \delta = 0.0$ and (b) $\beta = 0.3, \delta = 0.7$.

THERMAL STRESS INTENSITY IN AN EDGE-CRACKED STRIP

As shown previously, tensile thermal stresses exist at the low-temperature side of a strip with temperature-dependent material properties. Thus, an edge crack at the low-temperature side (shown in Figure 1) may propagate. In some cases, an interior crack may also cause a fracture of the strip. We are only concerned here with the edge crack problem. Since a temperature-dependent Young's modulus only affects the thermal stress slightly, we, therefore, take Young's modulus to be constant in the following analysis of a crack problem. The boundary value problem for the thermally loaded edge-cracked strip is

$$\nabla^2 \nabla^2 F + \frac{E_0}{\tau} \nabla^2 [\alpha(T - T_0)] = 0$$

$$\sigma_{11} = \sigma_{12} = 0 \quad x_1 = 0, b \quad x_2 \geq 0$$

$$\sigma_{12} = \sigma_{22} = 0 \quad 0 \leq x_1 \leq a \quad x_2 = 0$$

$$\sigma_{12} = v_2 = 0 \quad a < x_1 \leq b \quad x_2 = 0$$

where the temperature is given by Eq. (15), v_2 is the displacement in x_2 -direction, and a and b equal the crack length and the strip width, respectively.

Using the Fourier transform and the integral equation methods [15], the preceding boundary value problem is reduced to the singular integral equation

$$\int_{-1}^1 \left[\frac{1}{s-r} + K(r, s) \right] \phi(s) ds = - \frac{2\pi(1-\nu_0^2)}{E_0} \sigma_{22}^T \quad |r| \leq 1$$

where the unknown function $\phi(r)$ is given by

$$\phi(x_1) = \partial v_2(x_1, 0) / \partial x_1$$

and $K(r, s)$ is a known kernel singular only at $(r, s) = (-1, -1)$, $r = 2x_1/a - 1$. The function $\phi(r)$ can be further expressed as [15]

$$\phi(r) = \psi(r) / \sqrt{1-r}$$

where $\psi(r)$ is continuous and bounded on $[-1, 1]$. When $\phi(r)$ is normalized by $(1 + \nu_0)\alpha_0\Delta T$, the nondimensional *thermal stress intensity factor* (TSIF), K^* , at the crack tip is obtained as

$$K^* = \frac{(1-\nu_0)K_I}{E_0\alpha_0\Delta T\sqrt{\pi a}} = -\frac{1}{2}\psi(1)$$

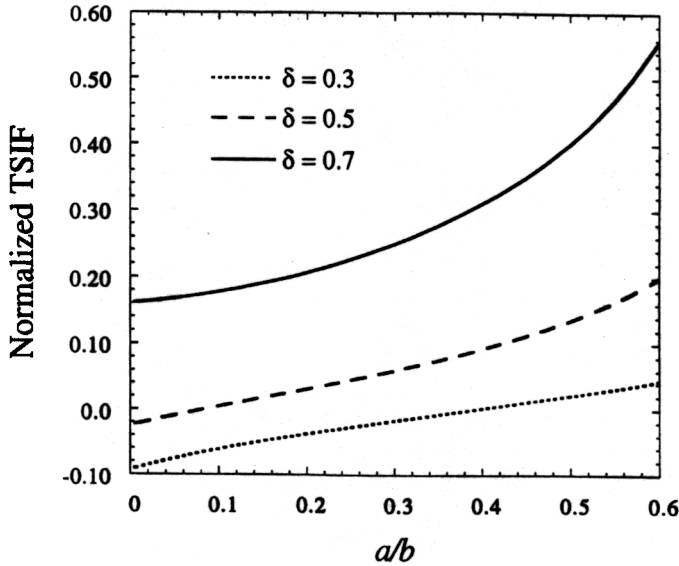


Figure 6. Normalized thermal stress intensity factor for $\delta = 0.3, 0.5, 0.7$ and $\gamma = 0.5, \beta = 0.0$.

Figure 6 shows the nondimensional TSIF versus the normalized crack length a/b for $\delta = 0.3, 0.5, 0.7$ and $(\gamma, \beta) = (0.5, 0.0)$. It can be seen that for $\delta = 0.7$, the TSIF is always positive and increases with increasing a/b . For $\delta = 0.3$ and 0.5 , the TSIF also increases with increasing a/b but is negative for $a/b < 0.09$ ($\delta = 0.5$) and $a/b < 0.38$ ($\delta = 0.3$). The negative TSIF means there is no crack-tip opening for those crack lengths and the crack will not grow. Figure 7 exhibits the TSIF for $\gamma = 0.1, 0.3, 0.5$ and $(\delta, \beta) = (0.7, 0.0)$. The TSIF is always positive for $\gamma = 0.3$ and 0.5 , but for $\gamma = 0.1$ the TSIF is negative for $a/b < 0.15$. For the example of Si_3N_4 considered in the previous section, the TSIFs for $a/b = 0.1$ and 0.2 are about $4.59 \text{ MPa}\sqrt{m}$ and $8.18 \text{ MPa}\sqrt{m}$, respectively. The latter far exceeds the fracture toughness (about $4 - 5 \text{ MPa}\sqrt{m}$) of the material. Note that the specimen is free from thermal stresses when the temperature dependence of material properties is not considered.

CRACK GROWTH RESISTANCE CURVE

It is well known that polycrystalline ceramics exhibit crack growth resistance (R -curve) behavior. Though there are several mechanisms of toughening, crack-face-grain-bridging perhaps contributes most to the toughness increase at least for coarse-grained ceramics [16–19]. When a crack has initiated, it will grow with

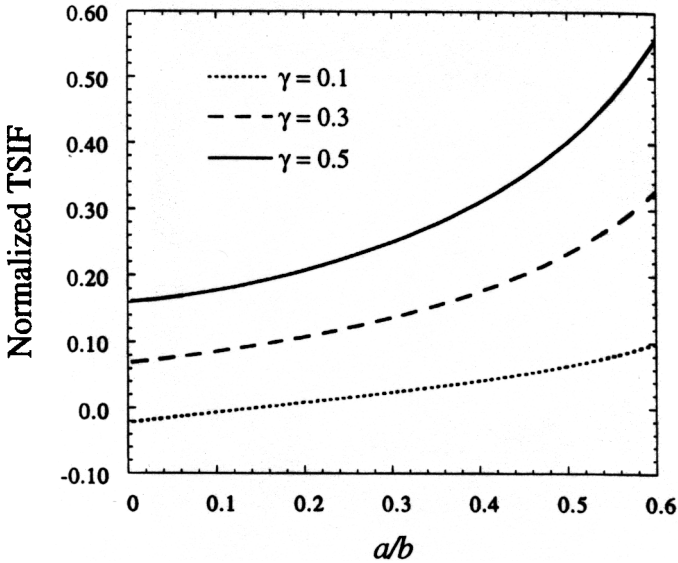


Figure 7. Normalized thermal stress intensity factor for $\gamma = 0.1, 0.3, 0.5$ and $\delta = 0.7, \beta = 0.0$.

grains bridging the crack faces. The grain bridging is characterized by the bridging law [18, 19]

$$\sigma = \sigma_m(1 - D/D_0)$$

where σ is the bridging stress, σ_m is the maximum bridging stress, D is the crack opening displacement, and D_0 is the maximum crack opening at which the bridging is lost. D_0 is usually related to grain size and, therefore, is temperature independent. Bower and Ortiz [18] argued that σ_m is due to compressive thermal residual stresses by which the grains are pinched to the matrix. When a ceramic is subjected to elevated temperatures, the thermal residual stress will be relaxed, which will reduce the bridging stress. We assume that the variation of the maximum bridging stress σ_m with temperature is given by

$$\sigma_m = \sigma_0[1 - \eta'(T - T_0)]^N$$

where σ_0 is the maximum bridging stress at $T = T_0$, N is an index, and η' is a constant that may be approximately taken to be the inverse of the processing temperature if we assume that the bridging is completely ineffective at the processing temperature. Equations (29) and (30) give the temperature-dependent bridging law as

$$\sigma = \sigma_0[1 - \eta'(T - T_0)]^N(1 - D/D_0)$$

THERMAL FRACTURE OF CERAMICS

Now consider an infinite strip of width b containing an edge crack subjected to remote bending moment M . The singular integral equation of the crack problem including the crack bridging law (31) is

$$\int_{-1}^1 \left[\frac{1}{s-r} + K(r,s) \right] \phi(s) ds - a_0^* \left(\frac{a}{a_0} \right) H(r-r_0) [1 - \eta'(T-T_0)]^N \int_r^1 \phi(s) ds$$

$$= \frac{2\pi(1-\nu_0^2)}{E_0} \left[-\sigma_b \left(1 - \frac{a}{b}(1+r) \right) + H(r-r_0) \sigma_0 (1 - \eta'(T-T_0))^N \right]$$

$|r| \leq 1$

where $H(\)$ is the Heaviside step function, $\sigma_b = 6M/b^2$, a_0 is the initial crack length, $a = a_0 + \Delta a$ is the total crack length, Δa is the crack growth, $r = 2x_1/a - 1$, $r_0 = 2a_0/a - 1$, and

$$a_0^* = \frac{2\pi a_0(1-\nu_0^2)}{E_0} \quad (33)$$

is a nondimensional parameter. In Eq. (32), the temperature $T(x_1)$ is for the specific problem being studied. In our example, T is given by Eq. (15). Hence, when the temperature dependence of crack bridging is considered, the R -curve will be influenced by the temperature distribution.

The integral equation (32) has a solution of the form

$$\phi(r) = \frac{\psi(r)}{\sqrt{1-r}} = \frac{1}{\sqrt{1-r}} \frac{1-\nu_0^2}{E_0} [\sigma_b \psi_1(r) + \sigma_0 \psi_2(r)]$$

where ψ_1 and ψ_2 are due to σ_b and σ_0 , respectively. The crack-tip stress intensity factor is

$$K_I = \sqrt{\pi a} \left[-\frac{1}{2} \psi_1(1) \sigma_b - \frac{1}{2} \psi_2(1) \sigma_0 \right] \quad (35)$$

The effective fracture toughness or the R -curve can be calculated from

$$K_R(a) = \sigma^c \sqrt{\pi a} \left(-\frac{1}{2} \psi^0(r) \right) \Big|_{r=1} \quad (36)$$

where $\psi^0(r) = \sqrt{(1-r)} \phi^0(r)$; $\phi^0(r)$ is the solution of Eq. (32) without considering bridging; and σ^c , the stress corresponding to $K_I = K_{IC}$, or the intrinsic fracture toughness of the material, is given by

$$\sigma^c = \frac{1}{-(1/2)\psi_1(1)} \left[\frac{K_{IC}}{\sqrt{\pi a}} + \frac{1}{2}\psi_2(1)\sigma_0 \right] \quad (37)$$

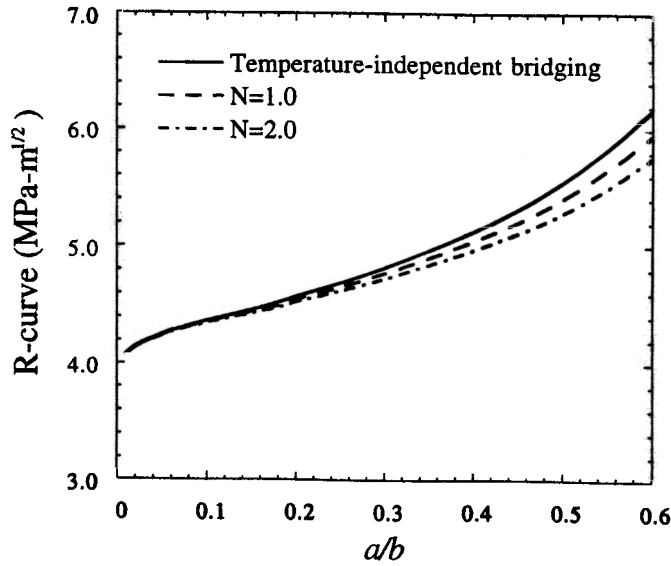
Here we assumed that the intrinsic toughness K_{IC} is a constant over the range of temperatures considered; K_{IC} may strongly depend on temperature, especially at high temperatures. For example, Mutoh et al. [20] found that the fracture toughness of silicon nitride decreases slightly with increasing temperature in the range 0–1200°C but strongly depends on temperatures above 1200°C.

Figures 8a, b depict the R -curve for the silicon nitride ceramic considered previously. The specimen width is taken to be 10 mm, and the two initial crack lengths considered are $a_0 = 0.05$ mm (Figure 8a) and 0.5 mm (Figure 8b). Values assigned to other parameters are $K_{IC} = 4$ MPa \sqrt{m} , $\sigma_0 = 6$ MPa, $D_0 = 10$ μm , $\eta' = 0.5 \times 800$ K $^{-1}$, and $N = 1.0$ and 2.0. In our calculations, we took T_0 as the room temperature 300 K and $\Delta T = 800$ K. It is observed that the R -curve is slightly weakened by considering temperature-dependent bridging. The crack also grows in the low temperature part of the specimen. It is expected that the effect of temperature-dependent bridging will be more pronounced for cracks in higher temperature environments.

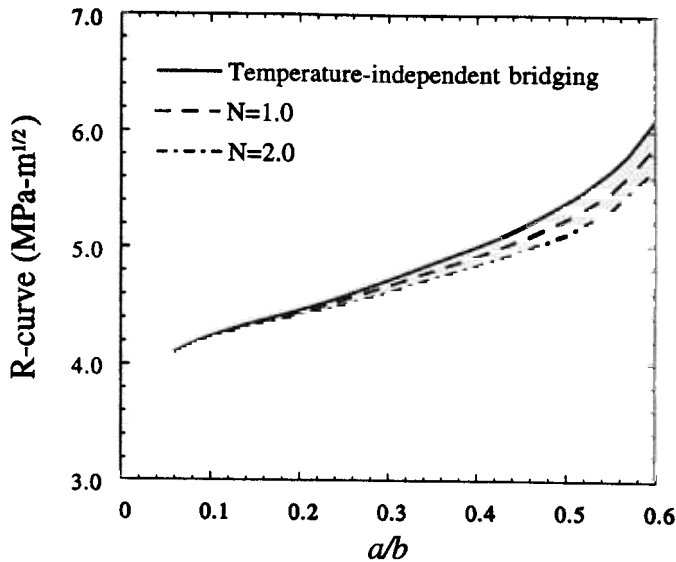
We now discuss crack growth instability in the sample specimen. Figure 9 shows both the R -curve ($a_0/b = 0.005$) and the stress intensity factor. It is known that ceramics exhibit subcritical crack growth behavior [21]. Under steady thermal loading conditions, a small crack will grow with time. When the crack length is smaller than about $a/b = 0.09$, the crack growth is stable and will become unstable once the crack length reaches about $a/b = 0.09$. When the temperature dependence of material properties is not considered, however, the crack will never grow under steady thermal loading because the specimen is free from thermal stresses.

CONCLUSIONS

We showed that the square-root singular field still prevails in the crack-tip region in materials with temperature-dependent properties. Hence, the stress intensity factor can still be used to study the fracture behavior of materials. The temperature dependence of material properties significantly affects thermal stresses and stress intensity factors in materials and structures subjected to high temperatures. The steady TSIF in an edge-cracked strip, which is zero when the temperature dependence of material properties is neglected, can reach and well exceed the fracture toughness of the ceramic when the temperature dependence of material properties is considered. Crack bridging, a major toughening mechanism in polycrystalline ceramics, may be degraded under high-temperature conditions. A temperature-dependent crack-bridging concept is proposed to study the R -curve behavior of ceramics at elevated temperatures.



(a)



(b)

Figure 8. Effect of temperature-dependent crack-bridging on R -curve of a ceramic: (a) $a_0/b = 0.005$ and (b) $a_0/b = 0.05$.

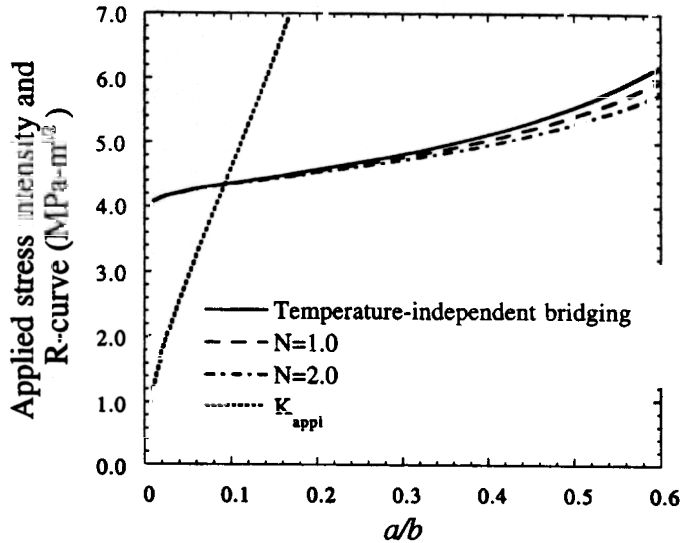


Figure 9. Crack growth instability in a ceramic.

REFERENCES

1. N. Noda, Thermal Stresses in Materials with Temperature-Dependent Properties, in R. B. Hetnarski (ed.), *Thermal Stresses I*, pp. 391–483, North-Holland, Amsterdam, 1986.
2. N. Noda, Thermal Stresses in Materials with Temperature-Dependent Properties, *Appl. Mech. Rev.*, vol. 44, pp. 383–397, 1991.
3. T. Hata, Thermoelastic Problem for a Griffith Crack in a Plate with Temperature-Dependent Properties under a Linear Temperature Distribution, *J. Thermal Stresses*, vol. 2, pp. 353–366, 1979.
4. T. Hata, Thermoelastic Problem for a Griffith Crack in a Plate Whose Shear Modulus Is an Exponential Function of the Temperature, *ZAMM*, vol. 61, pp. 81–87, 1981.
5. K. Kokini, Thermal Shock of a Cracked Strip: Effect of Temperature-Dependent Material Properties, *Engg. Fracture Mech.*, vol. 25, pp. 167–176, 1986.
6. Z.-H. Jin and N. Noda, Crack Tip Singular Fields in Nonhomogeneous Materials, *ASME J. Appl. Mech.*, vol. 61, pp. 738–740, 1994.
7. G. C. Sih, Heat Conduction in the Infinite Medium with Lines of Discontinuities, *ASME J. Heat Transfer*, vol. 87, pp. 293–298, 1965.
8. Z.-H. Jin and R. C. Batra, Some Basic Fracture Mechanics Concepts in Functionally Graded Materials, *J. Mech. Phys. of Solids*, vol. 44, pp. 1221–1235, 1996.
9. A. G. Evans and Y. Fu, Some Effects of Microcracks on the Mechanical Properties of Brittle Solids II: Microcrack Toughening, *Acta Meta.*, vol. 33, pp. 1525–1531, 1985.
10. M. Ortiz, A Continuum Theory of Crack Shielding in Ceramics, *ASME J. Appl. Mech.*, vol. 54, pp. 54–58, 1987.
11. M. Ortiz and A. E. Giannakopoulos, Mixed-Mode Crack Tip Fields in Monolithic Ceramics, *Int. J. Solids and Structures*, vol. 26, pp. 705–723, 1990.
12. J. F. Shackelford and W. Alexander, *The CRC Materials Science and Engineering Handbooks*, CRC Press, Boca Raton, FL, 1992.
13. Z.-H. Jin and R. C. Batra, Stress Intensity Relaxation at the Tip of an Edge Crack in a Functionally Graded Material Subjected to a Thermal Shock, *J. Thermal Stresses*, vol. 19, pp. 317–339, 1996.
14. B. K. Ganguly, K. R. McKinney, and D. P. H. Hasselman, Thermal Stress Analysis of a Flat Plate with Temperature-Dependent Thermal Conductivity, *J. Amer. Ceramic Soc.*, vol. 58, pp. 455–456, 1975.

15. G. D. Gupta and F. Erdogan, The Problem of Edge Cracks in an Infinite Strip, *ASME J. Appl. Mech.*, vol. 41, pp. 1001–1006, 1974.
16. P. L. Swanson, C. J. Fairbanks, B. R. Lawn, Y.-W. Mai, and B. J. Hockey, Crack Interface Grain Bridging as a Fracture Resistance Mechanism in Ceramics I: Experimental Study on Alumina, *J. Amer. Ceramic Soc.*, vol. 70, pp. 279–289, 1987.
17. G. Vekinis, P. W. R. Beaumont, and M. F. Ashby, R-Curve Behavior of Al_2O_3 Ceramics, *Acta Metal.*, vol. 38, pp. 1151–1162, 1990.
18. A. F. Bower and M. Ortiz, The Influence of Grain Size on the Toughness of Monolithic Ceramics, *ASME J. Engg. Mat. Tech.*, vol. 115, pp. 228–236, 1993.
19. Y.-W. Mai and B. R. Lawn, Crack Interface Grain Bridging as a Fracture Resistance Mechanism in Ceramics II: Theoretical Fracture Mechanics Model, *J. Amer. Ceramic Soc.*, vol. 70, pp. 289–294, 1987.
20. Y. Mutoh, N. Miyahara, K. Yamaishi, and T. Oikawa, Higher Temperature Fracture Toughness in Silicon Nitride and Sialon, *ASME J. Engg. Mat. Tech.*, vol. 115, pp. 268–272, 1993.
21. J. B. Wachtman, *Mechanical Properties of Ceramics*, John Wiley and Sons, New York, 1996.

APPENDIX

The scalars A_0 , A_{ij} ($i, j = 1, 2$) in Eq. (16) and \tilde{A}_0 , \tilde{A}_{ij} ($i, j = 1, 2$) and I_i ($i = 1, 2$) in Eq. (20) are

$$A_{11} = \int_0^b E' dx \quad A_{12} = \int_0^b E' x dx \quad A_{22} = \int_0^b E' x^2 dx$$

$$A_0 = A_{11}A_{22} - A_{12}^2 \quad E' = E/(1 - \nu^2)$$

and

$$\tilde{A}_{11} = \left[1 - \frac{1}{2}(\beta' + \delta')\Delta T + \frac{1}{3}\beta'\delta'(\Delta T)^2 \right] / \left(1 - \frac{1}{2}\delta'\Delta T \right)$$

$$\tilde{A}_{12} = \left[\frac{1}{2} - \frac{1}{3} \left(\frac{3}{2}\delta' + \beta' \right) \Delta T + \frac{1}{8}(\delta'^2 + 3\delta'\beta')(\Delta T)^2 - \frac{1}{10}\beta'\delta'^2(\Delta T)^3 \right]$$

$$\left(1 - \frac{1}{2}\delta'\Delta T \right)^{-2}$$

$$\tilde{A}_{22} = \left[\frac{1}{3} - \frac{1}{4}(\beta' + 2\delta')\Delta T + \frac{1}{5} \left(\frac{5}{4}\delta'^2 + 2\delta'\beta' \right) (\Delta T)^2 \right.$$

$$\left. - \frac{1}{24}(5\beta'\delta'^2 + \delta'^3)(\Delta T)^3 + \frac{1}{28}\beta'\delta'^3(\Delta T)^4 \right]$$

$$\left(1 - \frac{1}{2}\delta'\Delta T \right)^{-3}$$

$$\tilde{A}_0 = \tilde{A}_{11}\tilde{A}_{22} - \tilde{A}_{12}^2$$

$$I_1 = \left[\frac{1}{2} - \frac{1}{3}(\beta' + \delta' - \gamma')\Delta T + \frac{1}{4}(\beta'\delta' - \beta'\gamma' - \delta'\gamma')(\Delta T)^2 + \frac{1}{5}\beta'\delta'\gamma'(\Delta T)^3 \right]$$

$$\cdot \left(1 - \frac{1}{2}\delta'\Delta T\right)^{-1}$$

$$I_2 = \left[\frac{1}{3} - \frac{1}{4}\left(\beta' + \frac{3}{2}\delta' - \gamma'\right)\Delta T + \frac{1}{10}(3\beta'\delta' + \delta'^2 - 2\beta'\gamma' - 3\delta'\gamma')(\Delta T)^2 \right.$$

$$\left. + \frac{1}{12}(3\beta'\delta'\gamma' - \beta'\delta'^2 + \gamma'\delta'^2)(\Delta T)^3 - \frac{1}{14}\beta'\delta'^2\gamma'(\Delta T)^4 \right]$$

$$\cdot \left(1 - \frac{1}{2}\delta'\Delta T\right)^{-2}$$